

Spent-Coffee Grounds-Derived Biochar-Supported Heterogeneous Photocatalyst: A Performance Evaluation and Mechanistic Approach for the Degradation of Pentachlorophenol

Rahil Changotra^a, Himadri Rajput^a, Jie Yang^b, Mita Dasog^{*c}, Quan (Sophia) He^{*a}

^a*Department of Engineering, Faculty of Agriculture, Dalhousie University, Truro, NS B2N 5E3,
Canada*

^b*Institute of Oceanography, College of Geography and Oceanography, Minjiang University,
Fuzhou 350108, China*

^c*Department of Chemistry, Dalhousie University, Halifax, NS, B3H 4R2, Canada*

***Corresponding Authors:**

*Address: Professor, Department of Engineering, Faculty of Agriculture, Dalhousie University,
Truro, NS B2N 5E3, Canada (Q. He).*

*Associate Professor, Department of Chemistry, Dalhousie University, Halifax, NS, B3H 4R2,
Canada (M. Dasog).*

E-mail: quan.he@dal.ca (Q. He); mita.dasog@dal.ca (M. Dasog)

Text S1

Measurement of pH of Point of Zero Charges (pH_{PZC})

The measurement of pH of point of zero charges (pH_{PZC}) of the CGBT composite was determined with the following procedure: (1) a 25 mL sodium chloride (NaCl, 0.01 M) solution was placed into 60 mL glass bottle. The initial solution pH was adjusted to successive initial values between 2.0 and 12.0, and 0.05 g of the sample was added to the glass bottle. (2) The glass bottle was filled with N_2 to eliminate the effect of carbon dioxide (CO_2) on the pH change, and then shaken at 40 °C. (3) The final solution pH was measured after a desired contact time of 48 h. The difference between the final pH and the initial pH, denoted as ΔpH , was plotted against the initial pH. The solution pH at which the curve crosses the line of $\Delta \text{pH} = 0$ was taken as the pH_{PZC} of sample

Text S2

Description of quantum yield (QY), figure-of-merits (FOM), and space-time yield (STY)

Metrics based on the absorbed or incident irradiation and photon flux are crucial for evaluating catalytic systems for wastewater treatment. The literature has observed that a comparison has been made considering the conversion or degradation efficiencies under applied experimental conditions. However, a catalyst performing well under given experimental conditions may not necessarily provide optimal performance under variable conditions ¹. The comparative assessment of different systems based on conversion/degradation efficiency could not provide a meaningful comparison of actual performance. Consequently, there is an imperative need to perform the figure-of-merit based system performance that considers all the essential variables

in the catalytic processes. Besides, the performances of photocatalytic systems can be evaluated on a quantitative basis with the aid of diverse performance metrics such as the quantum yield (QY) and space-time yield (STY). Fundamentally, the QY of a reaction can be quantitatively determined by calculating the number of absorbed photons by the surface of the photocatalyst in a reaction using the equation (1) ².

$$QY = \frac{\text{Decay rate of pollutant (molecules per second)}}{\text{Photon flux (photons per second)}} \quad (1)$$

As the mass of photocatalyst is utilized in the reaction system, the process is different between different studies, space-time yield (STY) and figure-of-merit (FoM) are considered to normalize such effects, which are not considered in calculating QY ³. STY and FoM are also computed to assess the performance of the system using equations 2 and 3, respectively.

$$STY = \frac{QY \text{ (molecules per photon)}}{\text{Mass of catalyst (g)}} \quad (2)$$

$$FoM = \frac{\text{Conversion efficiency (\%)}}{\text{Mass of catalyst (g)} \times \text{Initial pollutant concentration (g L}^{-1}\text{)} \times \text{irradiation time (min)} \times \text{Power (W)}} \quad (3)$$

In the industrial sector, STY is defined as the net amount of product formation per unit time per packed volume of the catalyst bed ⁴. In our study, the STY concept can be considered as the quantitative analysis of the amount of organic contaminant degraded per unit time by a unit mass of catalyst. Our comparison of STY and FoM in conjunction with QY values provides judicious comparative performance among the different reaction systems employed and considers all associated variables in the reaction system. Accordingly, we compared our reaction system for

wastewater treatment with the other reported studies based on parameters such as irradiation light intensity and wavelength, a mass of catalyst, degradation and irradiation time, volume of the reaction medium, initial concentration, and molecular weight of the organic contaminant. All these parameters were used to compute the QY, STY and FoM values, and the results are compiled in Table S3.

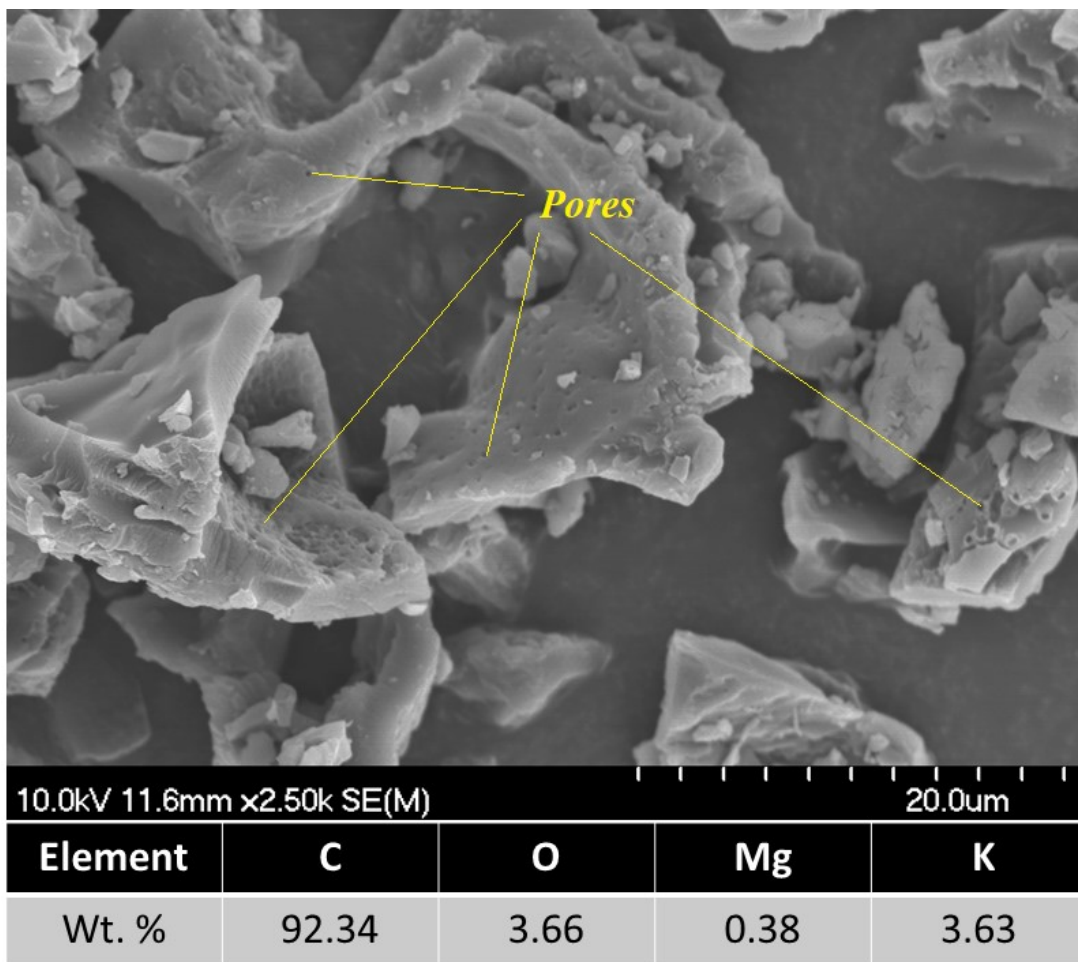


Fig. S1. SEM image of biochar and weight percentage of elements.

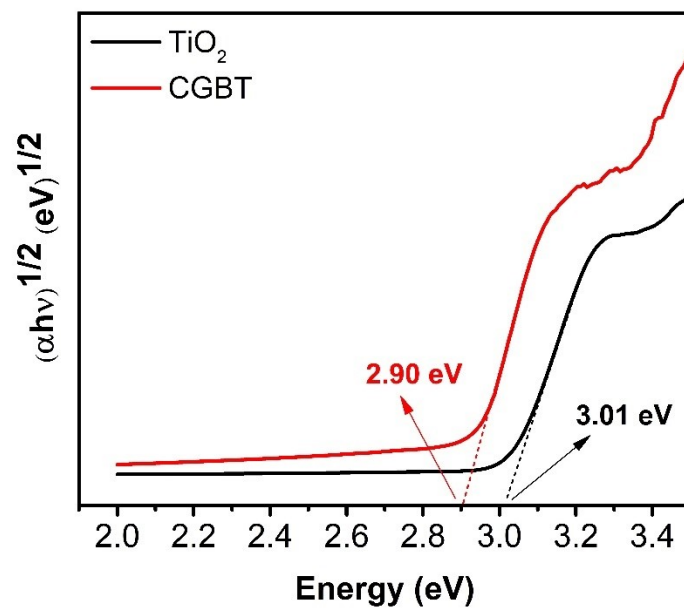


Fig. S2 Tauc plot of the synthesized photocatalysts

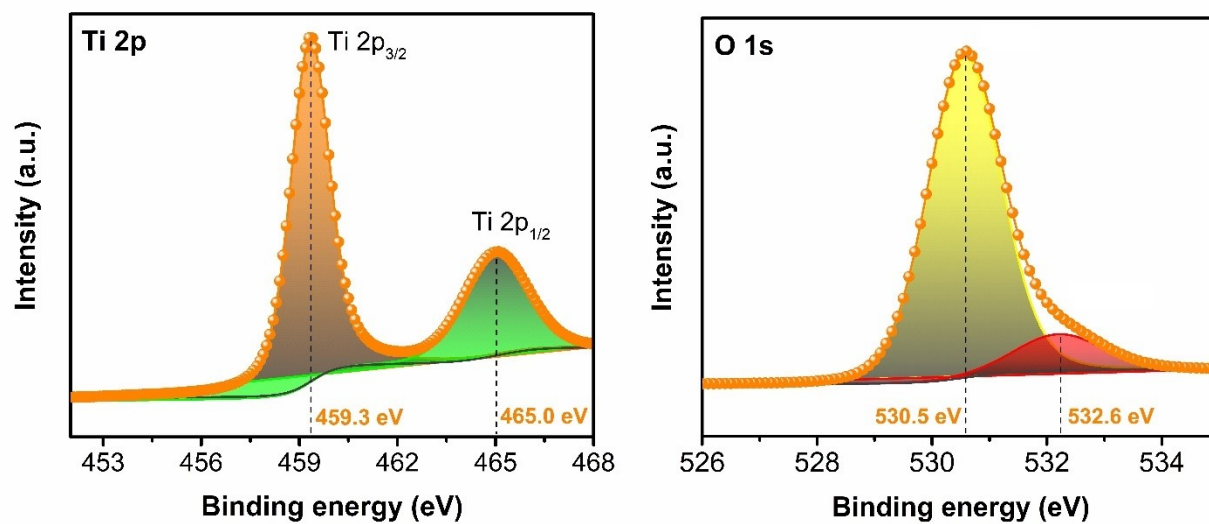


Fig. S3 High-resolution XPS Ti 2p and O 1s spectra of TiO₂ nanoparticles.

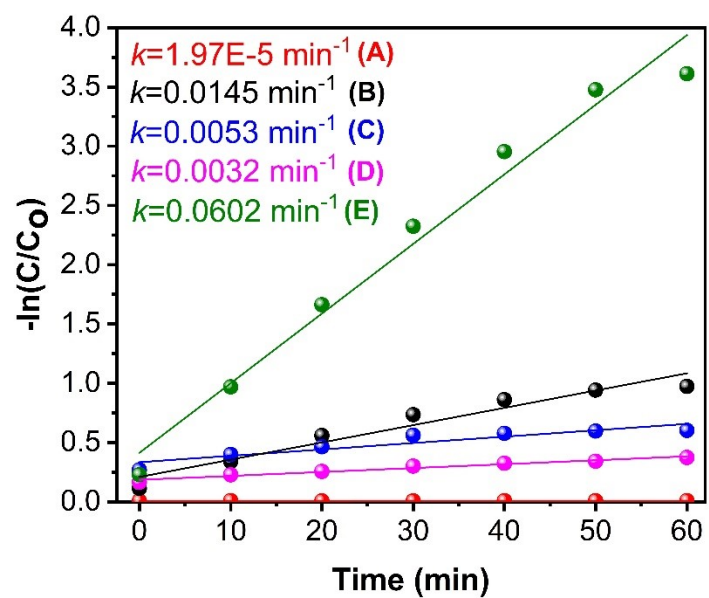


Fig. S4. Rate kinetics of photocatalytic degradation of PCP under photolysis (A) and in the presence of catalysts: TiO_2 (B), CGB (C), SCG (D), and CGBT (E) nanocomposite

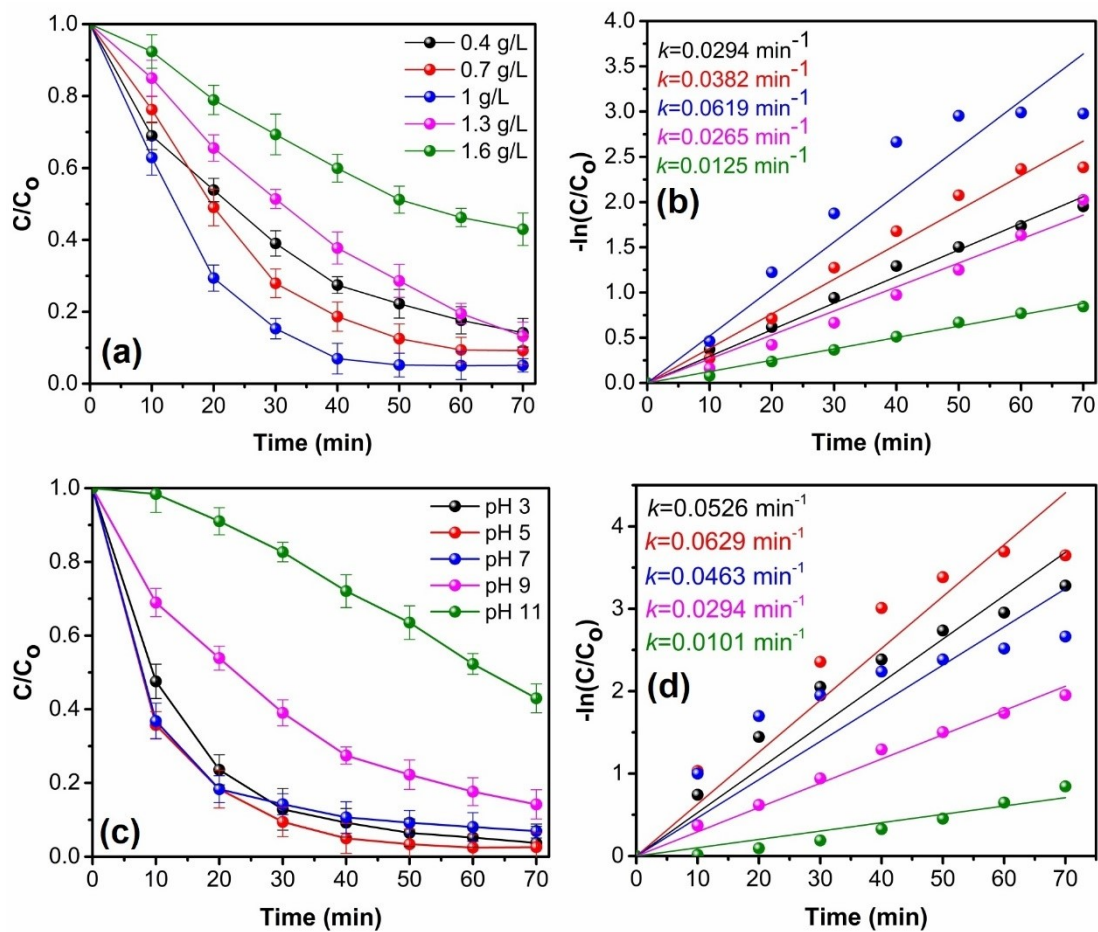


Fig. S5. (a) Effect of varying concentrations of CGBT nanocomposites on the photocatalytic degradation and (b) rate kinetics of PCP; (c) Effect of solution pH on the photocatalytic degradation and (d) rate kinetics of PCP (d) $[(PCP)_0] = 10 \text{ mg L}^{-1}$ and UV light irradiation)

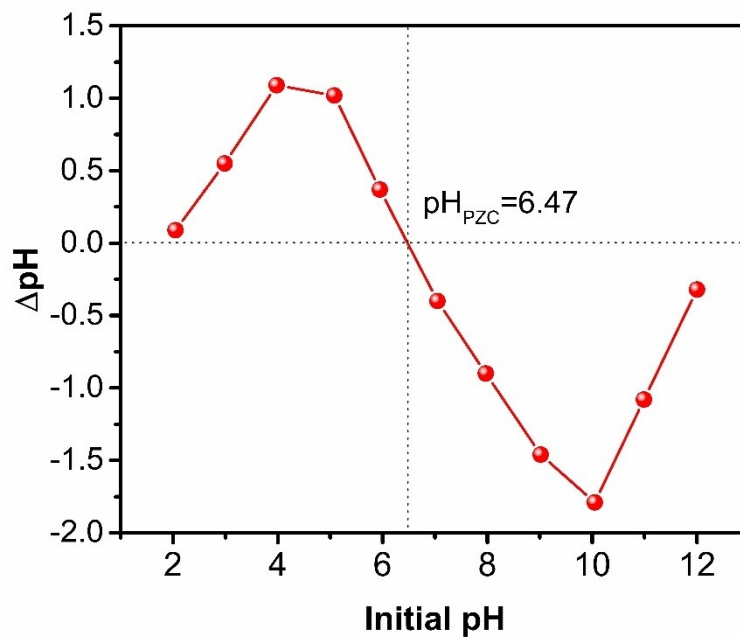


Fig. S6 Point of zero charge (pH_{PZC}) of CGBT nanocomposites.

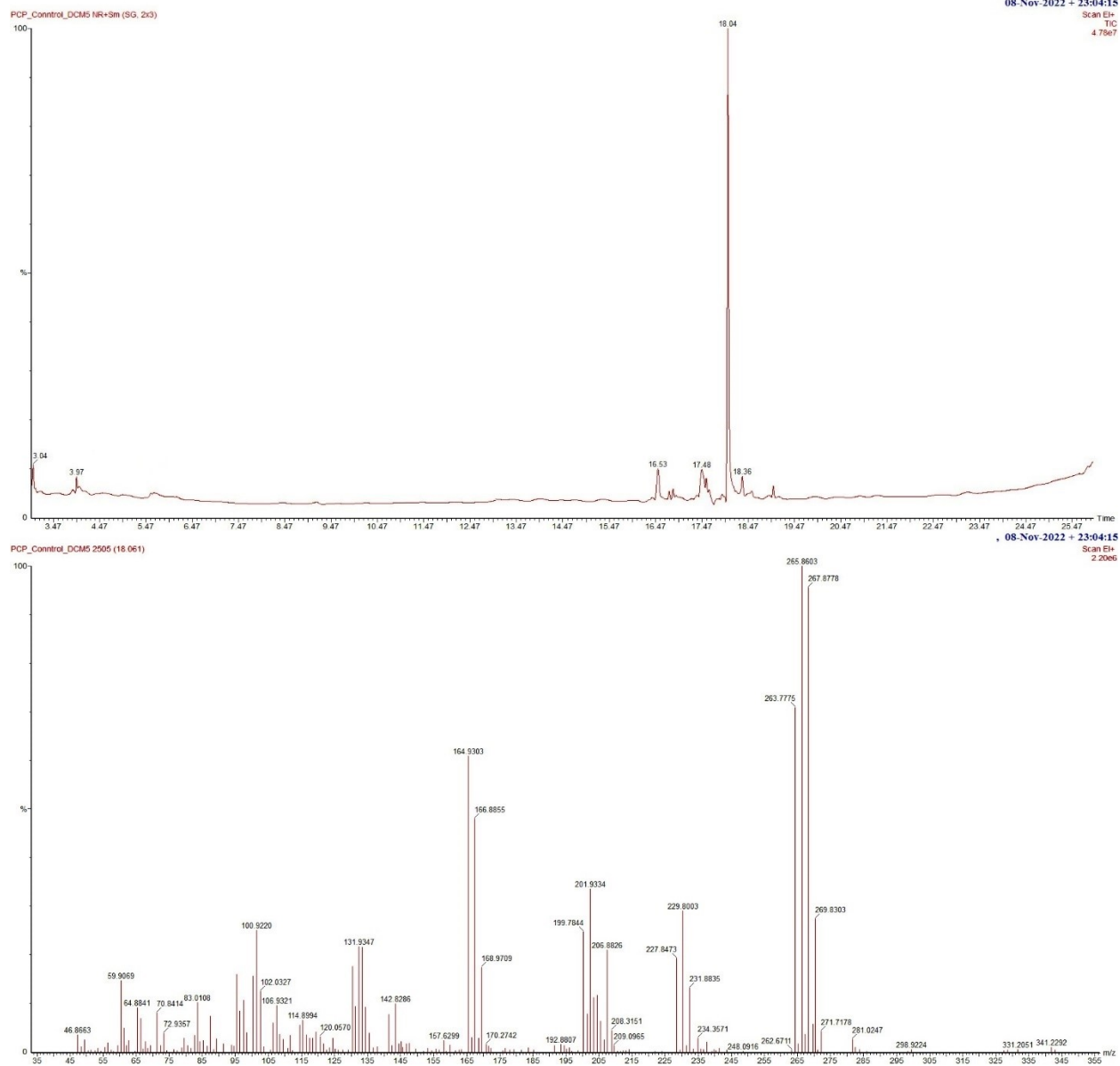


Fig. S7. GC chromatogram for PCP and mass spectra of PCP at $t_R=18.04$

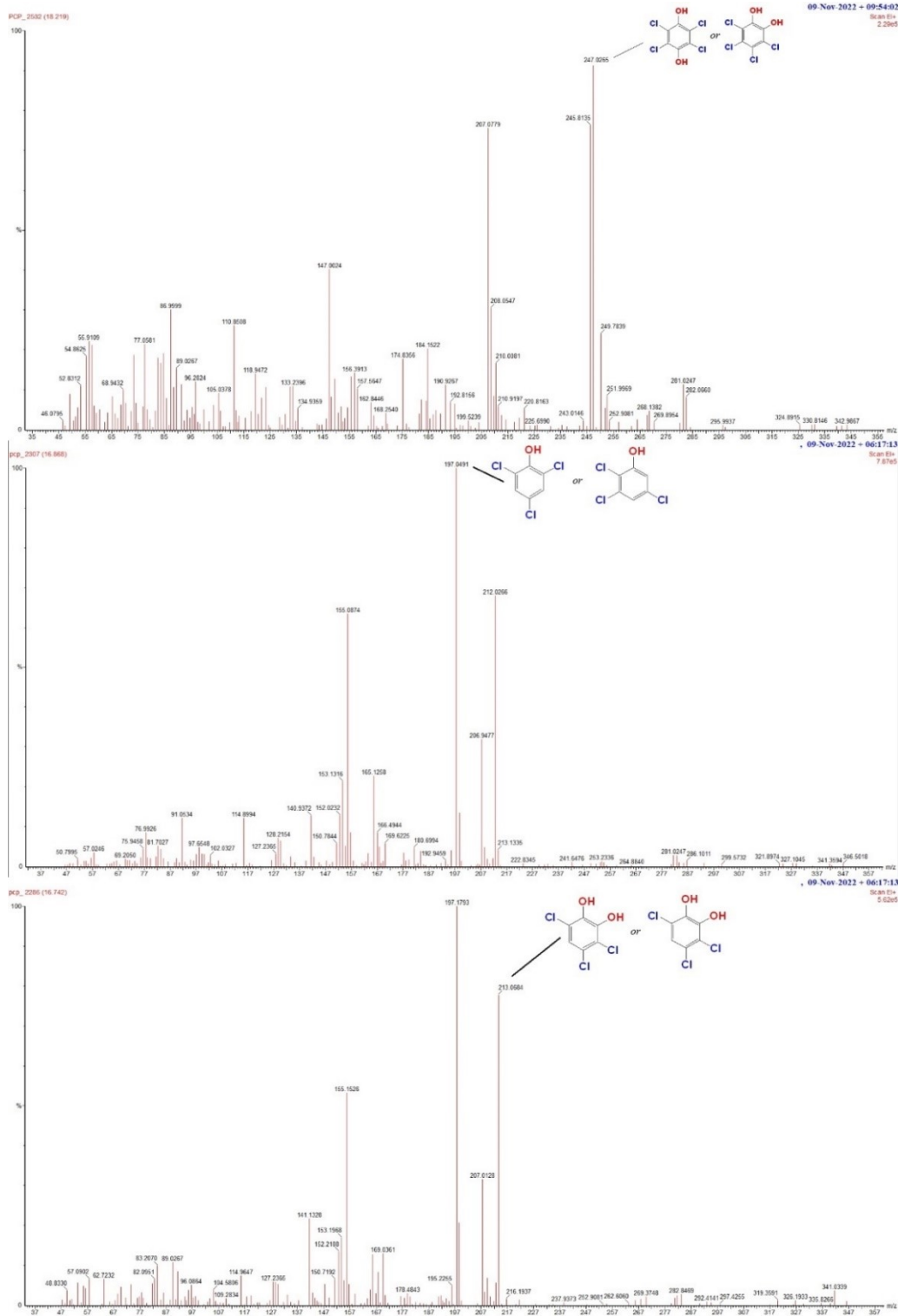


Fig. S8. Mass spectra of transformed products of PCP under photocatalytic degradation using CGBT nanocomposites.

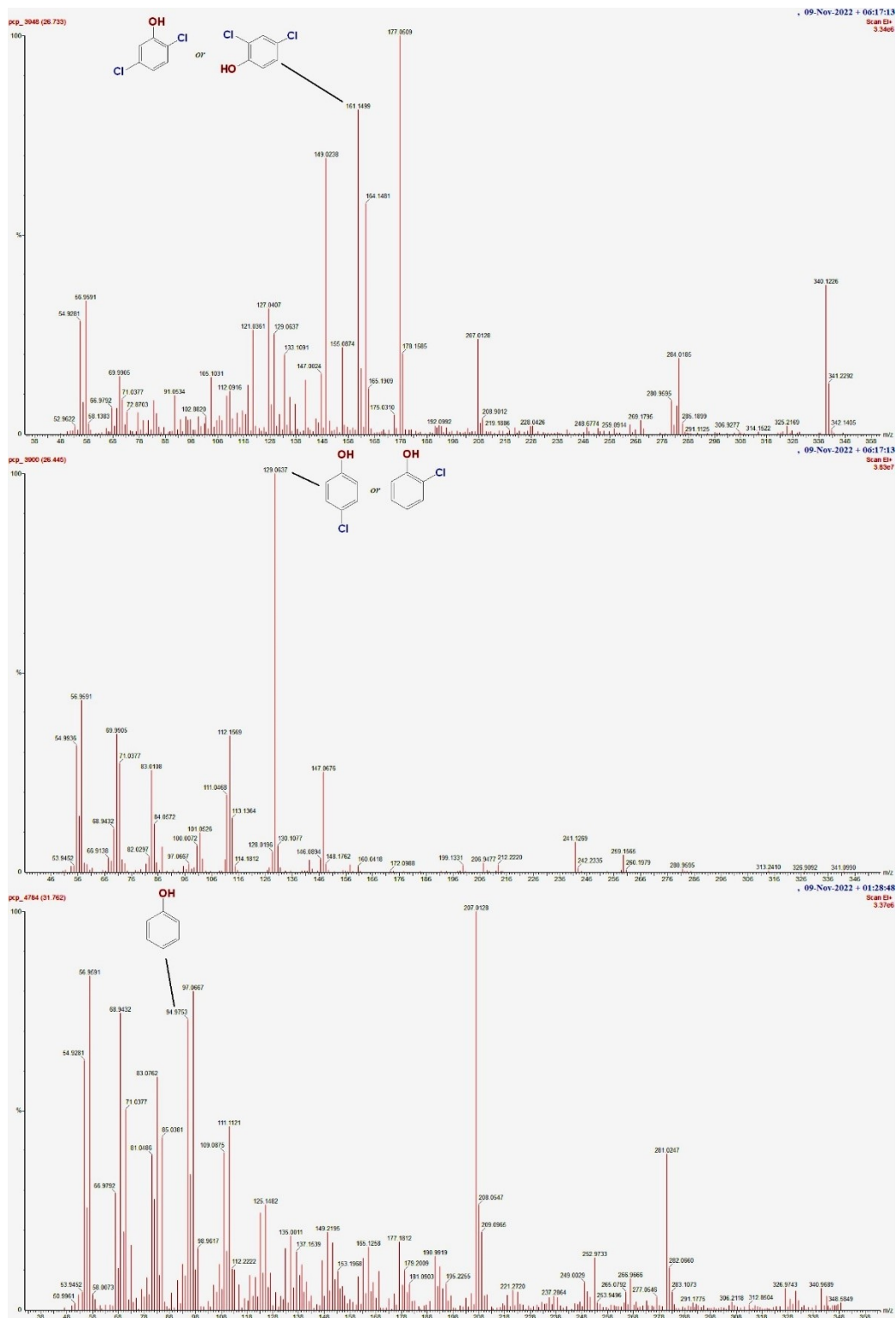


Fig. S9. Mass spectra of transformed products of PCP under photocatalytic degradation using CGBT nanocomposites.

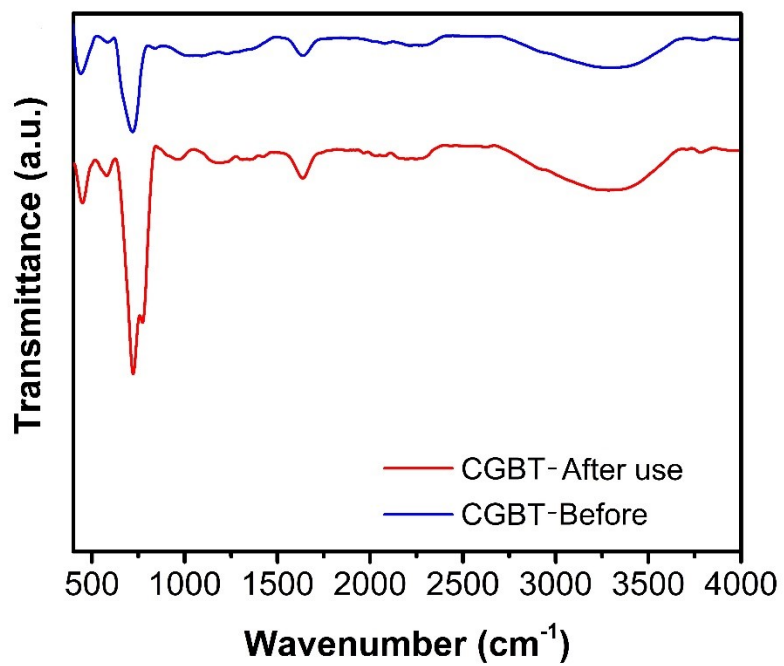


Fig. S10. FT-IR spectra of fresh and used CGBT nanocomposites after 5 consecutive cycles.

Table S1. Properties of pentachlorophenol

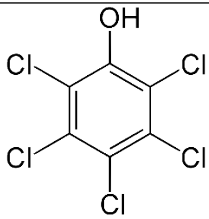
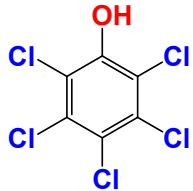
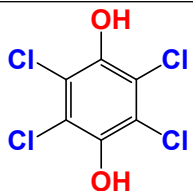
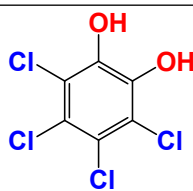
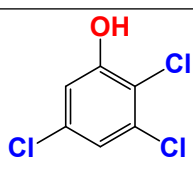
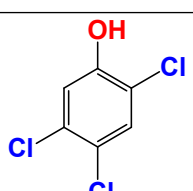
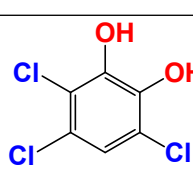
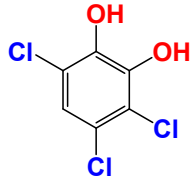
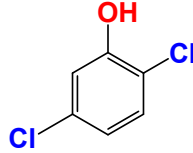
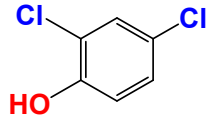
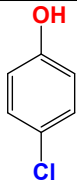
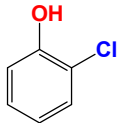
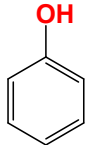
Name of clinical form	Pentachlorophenol
Molecular formula	C_6HCl_5O
Molecular weight	$266.34 \text{ g mol}^{-1}$
Aqueous solubility	0.020 g L^{-1} at $30 \text{ }^\circ\text{C}$
Chemical structure	

Table S2. Identified transformed products of pentachlorophenol by GC-MS

Substrate	Rt (min)	Chemical formula	Chemical structure	m/z fragments (% Similarity)
PCP	18.04	C ₆ HCl ₅ O		[M ⁺] 265.86 (100); 267.87 (90); 263.77 (70)
Tetrachloro- hydroquinone (TCHC)	18.21	C ₆ H ₂ Cl ₄ O ₂		[M ⁺] 247.02 (95); 245.81 (70); 249.78 (20)
Tetrachloro- pyrocatechol (TCPC)	18.21	C ₆ H ₂ Cl ₄ O ₂		[M ⁺] 247.02 (95); 245.81 (70); 249.78 (20)
2,3,5- trichlorophenol (TCP)	16.86	C ₆ H ₃ Cl ₃ O		[M ⁺] 197.04 (100)
2,4,5- trichlorophenol (TCP)	16.86	C ₆ H ₃ Cl ₃ O		[M ⁺] 197.04 (100)
3,5,6- trichloro-1,2- pyrocatechol	16.74	C ₆ H ₃ Cl ₃ O ₂		[M ⁺] 213.06 (80)

(TCPC)				
3,4,6-trichloro- 1,2- pyrocatechol (TCPC)	16.74	$C_6H_3Cl_3O_2$		$[M^+]$ 213.06 (80)
2,5- dichlorophenol (DCP)	26.73	$C_6H_4Cl_2O$		$[M^+]$ 161.14 (80); 164.14 (80); 165.19 (10)
2,4- dichlorophenol (DCP)	26.73	$C_6H_4Cl_2O$		$[M^+]$ 161.14 (80); 164.14 (80); 165.19 (10)
4-chlorophenol	26.44	C_6H_5ClO		$[M^+]$ 129.06 (100); 128.01 (10); 130.10 (10)
2-chlorophenol	26.44	C_6H_5ClO		$[M^+]$ 129.06 (100); 128.01 (10); 130.10 (10)
Phenol	31.72	C_6H_6O		$[M^+]$ 94.97 (65)
Ring opening products				

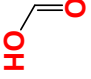
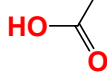
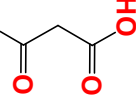
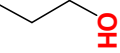
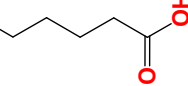
Formic acid	 <p>Chemical structure of formic acid (HCOOH) showing the carboxyl group in red.</p>
Acetic acid	 <p>Chemical structure of acetic acid (CH₃COOH) showing the carboxyl group in red.</p>
Malonic acid	 <p>Chemical structure of malonic acid (HOOC-CH₂-COOH) showing both carboxyl groups in red.</p>
1,3-Propanediol	 <p>Chemical structure of 1,3-propanediol (HO-CH₂-CH₂-CH₂-OH) showing both hydroxyl groups in red.</p>
Adipic acid	 <p>Chemical structure of adipic acid (HOOC-(CH₂)₄-COOH) showing both carboxyl groups in red.</p>

Table S3. Performance based comparison of our synthesized biochar-TiO₂ hybrid material with the reported biomass derived-TiO₂ photocatalysts and the photocatalyst utilized for the degradation of PCP.

Biomass derived-TiO ₂ photocatalysts						
Photocatalyst	Target pollutant	Experimental conditions*	QY# (molecule/ photon)	STY (molecules/ photon/g)	FoM (L/g/mol/J/h)	Ref.
Coffee-ground biochar-TiO ₂ (CGBT)	Pentachloro phenol (PCP)	C ₀ =10 mg/L; t = 60 min; pH 5; [Cat.] ₀ = 1 g/L; Light source: Hg lamps (UV light); t _{vol.} = 50 mL; Degradation=96.1%	3.07E-07	6.14E-06	3.24E-09	This study
Commercial TiO ₂	PCP	C ₀ =10 mg/L; t = 60 min; pH 5; [Cat.] ₀ = 1 g/L; Light source: Hg lamps (UV light); t _{vol.} = 50 mL; Degradation=49.3%	1.58E-07	3.15E-06	8.53E-10	This study
Synthesized TiO ₂	PCP	C ₀ =10 mg/L; t = 60 min; pH 5; [Cat.] ₀ = 1 g/L; Light source: Hg lamps (UV light); t _{vol.} = 50 mL; Degradation=57.8%	1.85E-07	3.70E-06	1.17E-09	This study

Soft wood pellets biochar-TiO ₂	Phenol	C _o =50 mg/L; t = 240 min; [Cat.] _o = 1 g/L; Light source: Hg lamps (UV light); t _{vol.} = 150 mL; Degradation=64.1%	7.94E-08	5.30E-07	5.59E-	5
TiO ₂ /Soft wood pellets carbon composite	Phenol	C _o =50 mg/L; t = 240 min; [Cat.] _o = 3.3 g/L; Light source: Hg lamps (UV light); t _{vol.} = 150 mL; Degradation=44.3%	5.49E-08	1.10E-07	8.01E-	6
Ag/TiO ₂ / walnut shell biochar	Methylene orange dye	C _o =20 mg/L; t = 60 min; [Cat.] _o = 0.25 g/L; Light source: Hg lamps (UV light); t _{vol.} = 40 mL; Degradation=97.4%	4.02E-08	4.02E-06	1.70E-	7
Peanut shells biochar/TiO ₂	Methylene blue dye	C _o =30 mg/L; t = 90 min; [Cat.] _o = 1 g/L; Light source: Hg lamps (UV light); t _{vol.} = 40 mL; Degradation=98%	2.72E-08	6.80E-07	2.92E-	8
TiO ₂ /Coconut shell biochar composite	Reactive Brilliant Blue	C _o =30 mg/L; t = 80 min; [Cat.] _o = 6 g/L; Light source: Hg lamps (UV light); t _{vol.} = 200 mL; Degradation=81.1%	2.18E-08	1.82E-08	3.24E-	9
TiO ₂ /Walnut shells biochar composite	Methylene orange dye	C _o =20 mg/L; t = 150 min; [Cat.] _o = 0.25 g/L; Light source: Hg lamps (UV light); t _{vol.} = 40 mL; Degradation=96.8%	6.39E-09	6.39E-07	2.68E-	10
Paper mill Sludge biochar-	Methylene orange dye	C _o =5 mg/L; t = 840 min; [Cat.] _o = 0.1 g/L; Light source: Hg lamps	6.14E-09	1.23E-06	5.86E-	11

TiO ₂ magnetic		(UV light); $t_{vol.} = 50$ mL; Degradation=87%				
Sugarcane bagasse biochar/H ₂ -TiO ₂	Enrofloxacin	$C_o=3.6$ mg/L; $t = 180$ min; [Cat.] _o =0.1 g/L; Light source: Xe lamps (Visible light); $t_{vol.} = 200$ mL; Degradation=95.6%	1.22E-09	6.08E-08	1.47E-	12
					10	
Macroalgae-based biochar/TiO ₂	Methylene blue dye	$C_o=5$ mg/L; $t = 240$ min; [Cat.] _o =2 g/L; Light source: Xe lamps (Visible light); $t_{vol.} = 50$ mL; Degradation=99.4%	7.02E-10	7.02E-09	4.41E-	13
					12	
TiO ₂ /Corn cob biochar composite	Sulfamethoxazole	$C_o=10$ mg/L; $t = 360$ min; pH 4; [Cat.] _o = 5 g/L; Light source: Hg lamps (UV-C); $t_{vol.} = 100$ mL; Degradation=91%	2.96E-10	5.91E-10	4.11E-	14
					13	
Photocatalysts for pentachlorophenol removal						
Ag ₂ CrO ₄	Sodium pentachlorophenate (PCP-Na)	$C_o=50$ mg/L; $t = 60$ min; pH 9.5; [Cat.] _o = 0.75 g/L; Light source: Xe lamps (Visible); $t_{vol.} = 200$ mL; Degradation=100%	1.98E-07	1.32E-06	3.34E-	15
					09	
Graphene- TiO ₂ nanocomposites	PCP-Na	$C_o=50$ mg/L; $t = 120$ min; [Cat.] _o = 0.2 g/L; Light source: Hg lamps (UV light); $t_{vol.} = 500$ mL; Degradation=97%	3.15E-08	3.15E-07	1.68E-	16
					09	
Vanadium-N-TiO ₂	PCP-Na	$C_o=20$ mg/L; $t = 120$ min; [Cat.] _o = 0.4 g/L; Light source: Xe lamps (Visible light); $t_{vol.} = 500$ mL;	3.11E-08	1.56E-07	8.05E-	17
					10	

			Degradation=82%			
Nanoporous Ti-doped β -Bi ₂ O ₃	PCP	C ₀ =10 mg/L; t = 60 min; pH 11.2; [Cat.] ₀ = 0.5 g/L; Light source: Xe lamps (Visible); t _{vol.} = 100 mL;	2.10E-08	4.21E-07	5.21E-10	18
			Degradation=98%			
Bi/SnO ₂ /TiO ₂ -graphene nanocomposite	PCP	C ₀ =20 mg/L; t = 120 min; pH 3; [Cat.] ₀ = 0.3 g/L; Light source: Hg lamps (UV light); t _{vol.} = 100 mL;	1.04E-08	3.46E-07	3.19E-10	19
			Degradation=84%			
Mesoporous TiO ₂ microspheres	PCP	C ₀ =10 mg/L; t = 135 min; pH 9; [Cat.] ₀ = 1 g/L; Light source: Hg lamps (UV-C light); t _{vol.} = 100 mL;	6.88E-09	6.88E-08	5.14E-11	20
			Degradation=98%			
N-F-TiO ₂	PCP	C ₀ =5 mg/L; t = 120 min; pH 5; [Cat.] ₀ = 0.5 g/L; Light source: Xe lamps (Visible light); t _{vol.} = 250 mL; Degradation=95%	4.42E-09	3.54E-08	1.06E-10	21
			Degradation=98%			
Ag/TiO ₂ nanoparticles	PCP	C ₀ =20 mg/L; t = 160 min; [Cat.] ₀ = 0.15 g/L; Light source: Hg lamps (UV light); t _{vol.} = 20 mL;	4.16E-09	1.66E-06	3.58E-10	22
			Degradation=98%			
Bi ₁₂ SiO ₂₀	PCP	C ₀ =4 mg/L; t = 120 min; pH 6.1; [Cat.] ₀ = 0.25 g/L; Light source: Xe lamp (Visible light); t _{vol.} =200 mL;	4.09E-09	8.17E-08	1.97E-10	23
			Degradation=95%			
FeNi ₃ /SiO ₂ /	PCP	C ₀ =10 mg/L; t = 120 min; pH 3;	3.62E-09	1.45E-08	9.14E-10	24

ZnO magnetic nanocomposite		[Cat.] _o = 0.5 g/L; Light source: Xe lamps (Visible light); t _{vol.} = 500 mL; Degradation=100%				11
Ag/TiO ₂ nanotubes	PCP	C _o =10 mg/L; t = 180 min; [Cat.] _o = 1 g/L; Light source: Xe lamps (Visible light); t _{vol.} = 500 mL; Degradation=99%	2.48E-09	4.96E-09	3.10E-	25
α-Fe ₂ O ₃ /ZnO composites	PCP	C _o =10 mg/L; t = 240 min; pH 9; [Cat.] _o = 1.5 g/L; Light source: Xe lamps (Visible light); t _{vol.} = 100 mL; Degradation=98%	1.31E-09	8.76E-09	1.08E-	26
Bi ₂ O ₃ /TiO _{2-x} B _x	PCP	C _o =10 mg/L; t = 300 min; [Cat.] _o = 1 g/L; Light source: Xe lamps (Visible light); t _{vol.} = 50 mL; Degradation=85%	3.65E-10	7.30E-09	3.92E-	27

C_o: Initial concentration of pollutants; t: treatment time; [Cat]_o: Catalyst dosage; Hg: Mercury; Xe: Xenon; t_{vol}: Treatment volume.

* In calculating the photon flux, light intensity (mW cm⁻²) was considered based on the reported in the cited studies and where not mentioned, the common conditions of 100 mW cm⁻² were assumed as a reference value for performance evaluation.

QY values were calculated based upon the peak wavelength of the light source reported in the cited papers. For the reference without specific wavelength information, the common UV light (λ=365 nm) and visible light (λ=420 nm) conditions were assumed as a reference value for performance evaluation.

References

1. R. Changotra, A. K. Ray and Q. He, *Advances in Colloid and Interface Science*, 2022, 102793.
2. R. Changotra and A. Dhir, *Chemical Engineering Journal*, 2022, **442**, 136201.
3. K. Vikrant, K.-H. Kim and A. Deep, *Applied Catalysis B: Environmental*, 2019, **259**, 118025.
4. G. J. Janz and S. C. Wait Jr, *The Journal of Chemical Physics*, 1955, **23**, 1550-1551.
5. P. Lisowski, J. C. Colmenares, O. Masek, W. Lisowski, D. Lisovytskiy, A. Kaminska and D. Łomot, *ACS Sustainable Chemistry & Engineering*, 2017, **5**, 6274-6287.
6. P. Lisowski, J. C. Colmenares, O. Mašek, W. Lisowski, D. Lisovytskiy, J. Grzonka and K. Kurzydłowski, *ChemCatChem*, 2018, **10**, 3469-3480.
7. R. Shan, L. Lu, J. Gu, Y. Zhang, H. Yuan, Y. Chen and B. Luo, *Materials Science in Semiconductor Processing*, 2020, **114**, 105088.
8. H. Luo, S. Yu, M. Zhong, Y. Han, B. Su and Z. Lei, *Journal of Alloys and Compounds*, 2022, **899**, 163287.
9. S. Zhang and X. Lu, *Chemosphere*, 2018, **206**, 777-783.
10. L. Lu, R. Shan, Y. Shi, S. Wang and H. Yuan, *Chemosphere*, 2019, **222**, 391-398.
11. C. P. Silva, D. Pereira, V. Calisto, M. A. Martins, M. Otero, V. I. Esteves and D. L. Lima, *Journal of Environmental Management*, 2021, **294**, 112937.
12. J. Shi, W. Huang, H. Zhu, J. Xiong, H. Bei and S. Wang, *ACS omega*, 2022, **7**, 12158-12170.
13. T. Fazal, A. Razzaq, F. Javed, A. Hafeez, N. Rashid, U. S. Amjad, M. S. U. Rehman, A. Faisal and F. Rehman, *Journal of hazardous materials*, 2020, **390**, 121623.
14. J. R. Kim and E. Kan, *Journal of environmental management*, 2016, **180**, 94-101.
15. Y. Liu, H. Yu, M. Cai and J. Sun, *Catalysis Communications*, 2012, **26**, 63-67.
16. Y. Zhang, Z. Zhou, T. Chen, H. Wang and W. Lu, *Journal of environmental sciences*, 2014, **26**, 2114-2122.
17. J. Liu, R. Han, Y. Zhao, H. Wang, W. Lu, T. Yu and Y. Zhang, *The Journal of Physical Chemistry C*, 2011, **115**, 4507-4515.
18. L. Yin, J. Niu, Z. Shen and J. Chen, *Environmental science & technology*, 2010, **44**, 5581-5586.
19. M. H. Sayadi, S. Homaeigohar, A. Rezaei and H. Shekari, *Environmental science and pollution research*, 2021, **28**, 15236-15247.
20. J. Xie, L. Bian, L. Yao, Y. Hao and Y. Wei, *Materials Letters*, 2013, **91**, 213-216.
21. M. Antonopoulou, D. Vlastos and I. Konstantinou, *Photochemical & Photobiological Sciences*, 2015, **14**, 520-527.
22. H. Zhang, C. Liang, J. Liu, Z. Tian, G. Wang and W. Cai, *Langmuir*, 2012, **28**, 3938-3944.
23. Y. Li, J. Niu, L. Yin, W. Wang, Y. Bao, J. Chen and Y. Duan, *Journal of Environmental Sciences*, 2011, **23**, 1911-1918.
24. F. S. Arghavan, A. Hossein Panahi, N. Nasseh and M. Ghadirian, *Environmental Science and Pollution Research*, 2021, **28**, 7462-7475.

25. L. Yu, X. Yang, Y. Ye, X. Peng and D. Wang, *Journal of colloid and interface science*, 2015, **453**, 100-106.
26. J. Xie, Z. Zhou, Y. Lian, Y. Hao, P. Li and Y. Wei, *Ceramics International*, 2015, **41**, 2622-2625.
27. K. Su, Z. Ai and L. Zhang, *The Journal of Physical Chemistry C*, 2012, **116**, 17118-17123.